Nonideal high-β magnetohydrodynamic Kelvin-Helmholtz instability driven by the shear in the ion diamagnetic drift velocity at the subsolar magnetopause

Akira Miura

Department of Earth and Planetary Science, University of Tokyo, Tokyo, Japan

Received 27 June 2002; revised 25 August 2001; accepted 26 November 2002; published 13 February 2003.

[1] A nonideal magnetohydrodynamic (MHD) Kelvin-Helmholtz (K-H) instability peculiar to a high-β plasma with a nonuniform pressure is studied for the magnetosheath field due north at the subsolar magnetopause, where the ideal MHD K-H instability driven by the shear in the $\mathbf{E} \times \mathbf{B}$ drift velocity is not operative. This instability is driven by the shear in the ion diamagnetic drift velocity, which is a nonideal MHD drift in a high-β plasma and is a macroscopic effect not visible at the guiding center level. The two-dimensional stability ($\mathbf{k} \cdot \mathbf{B}_0 = 0$) of a model subsolar magnetopause is investigated by solving the eigenmode equation for a polygonal ion diamagnetic drift velocity profile with the density ratio across the magnetopause as a parameter. Near the subsolar magnetopause the fastest growing wave or vortex propagates duskward with a phase velocity from 8 km/s to 14 km/s, and the normalized growth rate decreases with an increase in the ratio of the magnetosheath density to the magnetospheric density. The wavelength and period of the fastest growing mode increases with the density ratio. For realistic parameters near the subsolar magnetopause the wave period becomes 750 s to 2000 s and the wavelength becomes 11000 km to 16000 km. The present K-H instability ("diamagnetically driven K-H instability") may cause a plasma transport across the subsolar magnetopause, since the plasma motion is decoupled from that of the magnetic field owing to nonideal MHD. We discuss a possible dawn-dusk asymmetry (caused by the ion diamagnetic drift velocity at the magnetopause) of the K-H instability when the present instability is extended to the dayside magnetopause off the noon meridian, where the tailward $\mathbf{E} \times \mathbf{B}$ drift is no longer negligible. The vortex created by the present instability near the subsolar magnetopause has the same rotational sense as that created by the $\mathbf{E} \times \mathbf{B}$ shear driven K-H instability within the dusk flank boundary but has the opposite rotational sense to that created by the $\mathbf{E} \times \mathbf{B}$ shear driven K-H instability within the dawn flank boundary. *INDEX TERMS:* 2752 Magnetospheric Physics: MHD waves and instabilities; 2724 Magnetospheric Physics: Magnetopause, cusp, and boundary layers; 7859 Space Plasma Physics: Transport processes; 7863 Space Plasma Physics: Turbulence; 2784 Magnetospheric Physics: Solar wind/magnetosphere interactions; *KEYWORDS:* Kelvin-Helmholtz instability, nonideal MHD, high-beta plasma, ion diamagnetic drift velocity, plasma transport, subsolar magnetopause

Citation: Miura, A., Nonideal high-β magnetohydrodynamic Kelvin-Helmholtz instability driven by the shear in the ion diamagnetic drift velocity at the subsolar magnetopause, *J. Geophys. Res.*, *108*(A2), 1076, doi:10.1029/2002JA009563, 2003.

1. Introduction

[2] The hydromagnetic stability of high-β plasmas is relevant to the stability of a variety of regions in space plasmas. The magnetopause, which is a transition region from the shocked solar wind to the magnetosphere, is a high-β region. Let us assume that the magnetosheath field is due north and that the frozen-in law is valid. Then, the shear in the $\mathbf{E} \times \mathbf{B}$ drift velocity across the magnetopause in the dayside equatorial plane increases toward the flank magnetopause. Therefore the flank magnetopause is subject to the ideal magnetohydrodynamic (MHD) Kelvin-Helmholtz (K-H) instability driven by the shear in the $\mathbf{E} \times \mathbf{B}$ drift velocity, which was studied by *Chandrasekhar* [1961] using the frozen-in assumption ($\mathbf{E} + \mathbf{v} \times \mathbf{B} = \mathbf{0}$). A new K-H instability driven by the shear in the ion diamagnetic drift velocity, which is a nonideal MHD drift in a high-β plasma, was recently found [*Miura*, 2001]. This new instability is peculiar to the high-β MHD because the ion diamagnetic drift, which is an artifact of gyration, is not entirely the motion of guiding centers but is due to the magnetization and the ∇B drift averaged over a thermal distribution of velocities for a straight field line geometry. In this paper this new instability peculiar to the high-β plasma with a nonuniform pressure is applied to the subsolar magnetopause (stagnant point) for the magnetosheath field due north, where the conventional ideal MHD K-H instability driven by the $\mathbf{E} \times \mathbf{B}$ drift shear is not

0148-0227/03/2002JA009563$09.00

operative. Since the plasma pressure p_{st} just outside the subsolar magnetopause is given by $\sim \rho_{sw}v_{sw}^2$, where sw denotes the free stream solar wind, and the ion temperature is larger than the electron temperature, there is a large ion pressure gradient across the subsolar magnetopause. This causes the new K-H instability at the subsolar magnetopause. We include in the present study the density gradient at the magnetopause, which was not included in the previous analysis. Thus we can evaluate how the characteristics of unstable waves and vortices change with the density gradient at the subsolar magnetopause.

[3] It should be pointed out that the new K-H instability is obtained by using the generalized Ohm's law including the ∇p_e term and is essentially a nonideal MHD instability in a high-β plasma. There have been many studies investigating nonideal MHD and kinetic effects on the K-H instability, e.g., Hall MHD studies [*Opp and Hassam*, 1991; *Fujimoto and Terasawa*, 1991; *Huba*, 1994], hybrid MHD studies [*Thomas and Winske*, 1991, 1993; *Terasawa et al.*, 1992; *Fujimoto and Terasawa*, 1994] and kinetic studies [*Pritchett and Coroniti*, 1984; *Horton et al.*, 1987; *Tajima et al.*, 1991; *Wilber and Winglee*, 1995]. However, those studies considered $\mathbf{E} \times \mathbf{B}$ shear driven K-H instability in uniform plasmas or did not concentrate on the shear in the ion diamagnetic drift velocity and thus could not find a nonideal MHD instability driven by the shear in the ion diamagnetic drift velocity. Although there is a study of a K-H instability applied to the plasma sheet [*Yoon et al.*, 1996], which is not driven by the $\mathbf{E} \times \mathbf{B}$ drift shear, their Hall MHD analysis is applicable only to thin current sheets, where ions are unmagnetized, and therefore their model is applicable to a parameter regime different from the present study. The $\mathbf{E} \times \mathbf{B}$ shear driven K-H instability is important in the transport of momentum and energy in its nonlinear stage. The present diamagnetically driven K-H instability may cause a macroscopic anomalous transport of plasmas near the subsolar region because both ion and electron fluids in a vortex are not frozen-in to the magnetic field lines.

[4] The basic configuration for the present instability and the generalized Ohm's law used in this study are presented in section 2. The unperturbed state for the instability at the subsolar magnetopause is obtained in section 3. Dispersion equations and dispersion curves are obtained for a polygonal ion diamagnetic drift velocity profile in section 4. Characteristics of fastest growing waves and vortices are calculated for typical parameter sets near the subsolar magnetopause in section 5. A discussion is given in section 6. A summary is given in section 7.

2. Basic Configuration and the Generalized Ohm's Law

[5] We define a coordinate system, in which x is directed tailward, y is directed dawnward, and z is directed to the north. We consider a configuration in which the unperturbed magnetic field $\mathbf{B}_0(x)$ is in the z direction (due north), the unperturbed electric field $\mathbf{E}_0(x)$ is in the x direction, and the unperturbed pressure $p_0(x)$ and mass density $\rho_0(x)$ are functions of only x.

[6] The stability of the present configuration is described by the one-fluid MHD equations. Since the ion diamagnetic velocity near the subsolar point is much smaller than the fast magnetosonic speed, we assume the incompressibility. Instead of using the frozen-in law, we use the generalized Ohm's law,

$$-n\ e(\mathbf{E} + \mathbf{v} \times \mathbf{B}) + \mathbf{j} \times \mathbf{B} - \nabla p_e = 0, \tag{1}$$

which is derived from the equation of motion for the electron fluid by assuming that a timescale of our concern is much longer than the electron gyration period and that $\mathbf{v} \simeq \mathbf{v}_i$ and $\mathbf{j} = n\ e\ (\mathbf{v}-\mathbf{v}_e)$. Here n is the plasma density, p_e is the electron pressure, $\mathbf{v}$ is the macroscopic velocity of the plasma, and $\mathbf{v}_i$ and $\mathbf{v}_e$ are the average velocities of ion species and electron species, respectively.

3. Unperturbed State

[7] The unperturbed form of equation (1) can be written as

$$-n_0\ e(\mathbf{E}_0 + \mathbf{v}_0 \times \mathbf{B}_0) + \mathbf{j}_0 \times \mathbf{B}_0 - \nabla p_{e0} = 0 \tag{2}$$

where the subscript 0 denotes the unperturbed state. From the one dimensional assumption of the unperturbed state (only x-dependent) and $\nabla \cdot \mathbf{v}_0 = 0$, we obtain $v_{0x} = 0$, and we can assume $\mathbf{v}_0(x) = V_0(x)\ \hat{\mathbf{y}}$, where $\hat{\mathbf{y}}$ is the unit vector in the y direction. Then we obtain from the equation of motion

$$\mathbf{j}_0 \times \mathbf{B}_0 = \nabla p_0. \tag{3}$$

Thus one obtains from equations (2) and (3)

$$\mathbf{v}_{0\perp} = \frac{\mathbf{E}_0 \times \mathbf{B}_0}{B_0^2} + \frac{1}{n_0 e B_0^2}\mathbf{B}_0 \times \nabla p_{i0}, \tag{4}$$

where p_{i0} is the unperturbed ion pressure. Notice that the second term (ion diamagnetic drift velocity) which is essential for the present new K-H instability, should be absent in the ideal MHD. Using $\mathbf{b} = \mathbf{B}_0/B_0$ the ion diamagnetic drift velocity $\mathbf{V}_{di}$ is written as

$$\mathbf{V}_{di} = \frac{1}{n_0 e B_0}\mathbf{b} \times \nabla p_{i0}. \tag{5}$$

It is important to notice here that the ion diamagnetic drift velocity does not arise from the guiding center motion but can be expressed by using the magnetization of ion species $\mathbf{M}_i = -\mathbf{b}p_{i0}/B_0$ for an isotropic pressure in a following way [e.g., *Hazeltine and Waelbroeck*, 1998]. Since we have a vector identity

$$\nabla \times \mathbf{M}_i = \frac{1}{B_0}\mathbf{b} \times \nabla p_{i0} - p_{i0}\mathbf{b} \times \frac{1}{B_0^2}\nabla B_0 \tag{6}$$

for the present straight field line geometry, we obtain

$$e n_0 \mathbf{V}_{di} = e n_0 \mathbf{V}_{gci} + \nabla \times \mathbf{M}_i, \tag{7}$$

where

$$n_0 \mathbf{V}_{gci} \equiv \int d^3v f_i \mathbf{v}_{gci} \tag{8}$$

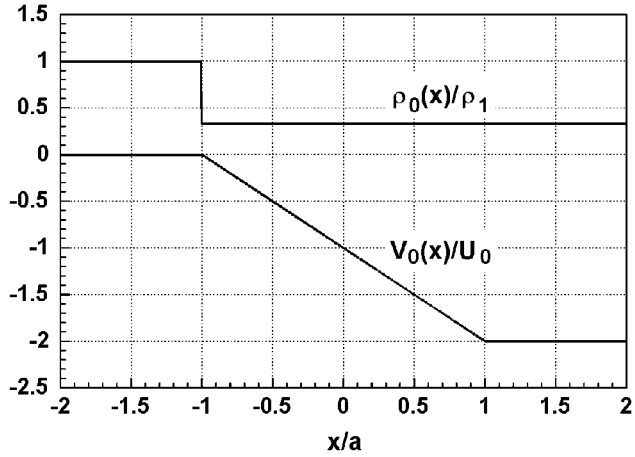

Figure 1. The profiles of $\rho_0(x)/\rho_1$ when $\rho_1/\rho_2 = 3.0$ and $V_0(x)/U_0$.

and $\mathbf{v}_{gci}$ is the ∇B drift velocity of an ion with a thermal distribution of the velocity characterized by the velocity distribution function f_i. The equation (7) means that although the diamagnetic drift is an artifact of gyration, it is a macroscopic effect, not visible at the guiding center level. Even if the guiding center is motionless, a net flow velocity can arise owing to the non-cancellation of the particle fluxes due to gyromotions of neighboring particles (the second term in the right hand side of equation (7)).

[8] The importance of the electric field term, i.e., the first term of equation (4), in considering the macroscopic velocity of space and cosmic plasmas, has been emphasized [*Alfvén*, 1954], a typical example in the magnetospheric physics being the "magnetospheric convection." However, the important implication of equation (4) is that in high-β space plasmas such as the subsolar region and the near-Earth plasma sheet, the ion diamagnetic drift velocity, i.e., the second term of equation (4), also becomes important, although this term is usually neglected assuming cold plasma approximation.

[9] From equation (3) and the Ampere's law we obtain

$$\frac{d}{dx}\left[p_0(x) + \frac{B_0^2(x)}{2\mu_0}\right] = 0. \tag{9}$$

Since we are considering the subsolar magnetopause, we assume that the frozen-in flow is zero, i.e., $\mathbf{E}_0 = E_0(x)\hat{\mathbf{x}} = 0$ and $V_0(x)$ is given solely by the ion diamagnetic drift velocity as follows:

$$V_0(x) = \frac{1}{n_0(x)eB_0(x)}\frac{dp_{i0}}{dx}. \tag{10}$$

We consider a particular case, where $p_{i0}(x)$ is proportional to the total pressure $p_0(x)$, i.e, $p_{i0}(x) = K\,p_0(x)$, where $K = T_{i0}/(T_{i0} + T_{e0})$, T_{i0} and T_{e0} being the unperturbed ion and electron temperatures, respectively. Near the subsolar magnetopause K is typically 0.8. Then we obtain

$$V_0(x) = -\frac{K}{\mu_0 n_0 e}\frac{dB_0}{dx}, \tag{11}$$

where equation (9) was used. For analytical tractability we use as a specific profile of $V_0(x)$ as shown in Figure 1, i.e.,

$$V_0(x) = \left\{ \begin{array}{cc} 0 & x \le -a \\ -U_0(x/a + 1) & |x| < a \\ -2U_0 & x \ge a \end{array} \right\}. \tag{12}$$

Here, $x = -a$ is the outer boundary of the magnetopause and $U_0 > 0$ is a constant velocity, which is given by $U_0 = [K/2\mu_0 n_0(x = a)e][dB_0/dx]_{x = a}$, where $x = a$ lies in the magnetosphere. Since there is a large density gradient across the magnetopause, we assume that the mass density $\rho_0(x) = \rho_1$ in $x \le -a$ and $\rho_0(x) = \rho_2$ in $x > -a$. Figure 1 shows the profile of $\rho_0(x)/\rho_1$ when $\rho_1/\rho_2 = 3.0$. From equation (11) one obtains

$$B_0(x) = -\frac{\mu_0 n_0 e}{K}\int_{x_0}^{x} V_0(x)dx + B_0(x_0). \tag{13}$$

[10] Figure 2 shows the profile of $B_0(x)$ normalized by $B_0(x_0)$, which is obtained from equation (13) by assuming $x_0 = -2a$, which lies in the magnetosheath, and $dB_0/dx = -(\mu_0/B_0)dp_0/dx = B_0(x_0)/(6a)$ at $x = a$. Once $B_0(x)$ is obtained, $p_0(x)$ can be obtained from equation (9) as follows:

$$p_0(x) = \frac{B_0^2(x_0)}{2\mu_0}\left[\beta(x_0) + 1 - \frac{B_0^2(x)}{B_0^2(x_0)}\right] \tag{14}$$

where β is the plasma beta value. Figure 2 shows the profile of $2\mu_0 p_0(x)/B_0^2(x_0)$, where we assumed $\beta(x_0) = 2\mu_0 p_0(x_0)/B_0^2(x_0) = 1.0$ as a typical value of the subsolar magnetosheath [*Eastman and Hones*, 1979]. Although not shown, the unperturbed temperature profile $T_0(x)$ can be determined from the fact that $p_0(x)$ is proportional to $\rho_0(x)T_0(x)$. Since there is a discontinuous drop of ρ_0 at $x = -a$, there should be a discontinuous jump of T_0 at $x = -a$, so as to make the pressure p_0 constant across $x = -a$. Since the plasma density is considered to be constant in $x > -a$ in the present model, the gradual pressure decrease toward the Earth,

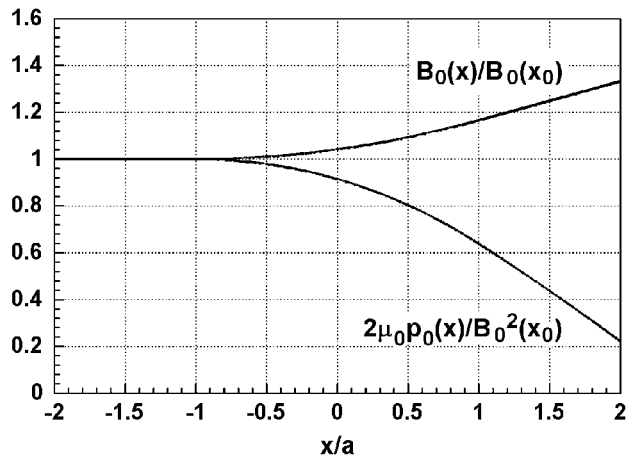

Figure 2. The profiles of $B_0(x)/B_0(x_0)$ and $2\mu_0 p_0(x)/B_0^2(x_0)$.

shown in Figure 2, is considered to be due to a gradual temperature decrease.

4. Dispersion Equations and Dispersion Curves

[11] We assume a two-dimensional (2-D) perturbation, which has no variation in the z direction ($\mathbf{k} \cdot \mathbf{B}_0 = 0$) and has the form $\delta f(x) \exp[i(ky-\omega t)]$. Since a temporal growth of the instability is considered, k is real and ω is complex. When the density is nonuniform, the eigenmode equation for the x component of the velocity perturbation δv_x becomes [*Miura*, 2001]

$$\frac{d^2\delta v_x}{dx^2} - \left(k^2 - \frac{k}{\omega - kV_0}\frac{d^2V_0}{dx^2}\right)\delta v_x + \frac{1}{\rho_0}\frac{d\rho_0}{dx}\left(\frac{d\delta v_x}{dx} + \frac{k}{\omega - kV_0}\frac{dV_0}{dx}\delta v_x\right) = 0, \tag{15}$$

where $V_0(x)$ is given by equation (10) in the present simplified model. In general, $V_0(x)$ is given by the sum of the $\mathbf{E} \times \mathbf{B}$ drift and the ion diamagnetic drift as given by equation (4). This means that the ion diamagnetic drift and the $\mathbf{E} \times \mathbf{B}$ drift for a fluid contribute the same way to the velocity shear and thus to the K-H instability. The equation (15) is similar to the eigenmode equation for the hydrodynamic case [*Chandrasekhar*, 1961]. However, the important difference is that in the present case $V_0(x)$ contains the diamagnetic drift velocity given by equation (10), which is peculiar to the high-β plasma and has no counterpart in hydrodynamics. We note that at both or either of $x = \pm a$, dV_0/dx and ρ_0 are discontinuous.

[12] There are two conditions at $x = \pm a$ imposed on the perturbation δv_x. One condition is that the x component of the displacement vector ξ_x is continuous at the interface. Since $d\xi_x/dt = \delta v_x$, the displacement ξ_x is given by

$$\xi_x = \frac{i}{\omega - kV_0}\delta v_x. \tag{16}$$

Since $V_0(x)$ is continuous at $x = \pm a$, δv_x must also be continuous at $x = \pm a$. The other condition is obtained by writing equation (15) as follows;

$$\frac{d}{dx}\left\{\rho_0\left[(\omega - kV_0)\frac{d\delta v_x}{dx} + k\frac{dV_0}{dx}\delta v_x\right]\right\} = \rho_0 k^2(\omega - kV_0)\delta v_x. \tag{17}$$

We integrate equation (17) from $x = x_i - \varepsilon$ to $x = x_i + \varepsilon$, where $x_i = \pm a$, and take a limit of $\varepsilon \to 0$ ($\varepsilon > 0$). Since the right-hand side of equation (17) is a finite quantity, the integration of the right-hand side of equation (17) vanishes for $\varepsilon \to 0$. Therefore that condition at $x = x_i$ becomes

$$\left[\rho_0\left\{(\omega - kV_0)\frac{d\delta v_x}{dx} + k\frac{dV_0}{dx}\delta v_x\right\}\right]_{x_i-\varepsilon}^{x_i+\varepsilon} = 0 \tag{18}$$

for $\varepsilon \to 0$, which means the continuity of the quantity inside the bracket at $x = \pm a$.

[13] In each of three regions, i.e., $x < -a$, $|x| < a$, and $x > a$, $d\rho_0/dx = 0$ and $d^2V_0/dx^2 = 0$. Therefore in each region the eigenmode equation (15) becomes

$$\frac{d^2\delta v_x}{dx^2} - k^2\delta v_x = 0. \tag{19}$$

Since δv_x must vanish when $|x| \to \infty$, we must suppose that

$$\delta v_x = \begin{cases} Ae^{kx} & x \le -a \\ Be^{-kx} + Ce^{kx} & |x| < a \\ De^{-kx} & x \ge a \end{cases}, \tag{20}$$

where A, B, C, and D are arbitrary constants. From the continuity of δv_x at $x = \pm a$, we obtain

$$Ae^{-ka} = Be^{ka} + Ce^{-ka} \tag{21}$$

$$De^{-ka} = Be^{-ka} + Ce^{ka}. \tag{22}$$

From the condition in equation (18) at $x = \pm a$, we obtain

$$\rho_1\omega Ae^{-ka} = \rho_2\left[\omega\left(-Be^{ka} + Ce^{-ka}\right) - (U_0/a)\left(Be^{ka} + Ce^{-ka}\right)\right] \tag{23}$$

$$\rho_2\left[(\omega + 2kU_0)\left(-Be^{-ka} + Ce^{ka}\right) - (U_0/a)\left(Be^{-ka} + Ce^{ka}\right)\right] = -\rho_2(\omega + 2kU_0)De^{-ka}. \tag{24}$$

[14] By deleting A, B, C, and D from equations (21)–(24) and after some algebra we obtain a dispersion equation determining ω;

$$\omega^2 + 2kU_0\left[1 - \frac{(\alpha - 1)}{4(\alpha + 1)ka}\left(1 - e^{-4ka}\right)\right]\omega + \frac{2(kU_0)^2}{(\alpha + 1)ka}\left[1 - \frac{1}{4ka}\left(1 - e^{-4ka}\right)\right] = 0, \tag{25}$$

where $\alpha = \rho_1/\rho_2$. When equation (25) has an unstable solution, ω_r and the growth rate γ, where $\omega = \omega_r + i\gamma$, are obtained from equation (25) as

$$\frac{\omega_r}{kU_0} = -\left[1 - \frac{(\alpha - 1)}{4(\alpha + 1)ka}\left(1 - e^{-4ka}\right)\right] \tag{26}$$

$$\left(\frac{\gamma}{kU_0}\right)^2 = -\left\{\left[1 - \frac{(\alpha - 1)}{4(\alpha + 1)ka}\left(1 - e^{-4ka}\right)\right]^2 - \frac{2}{(\alpha + 1)ka}\left[1 - \frac{1}{4ka}\left(1 - e^{-4ka}\right)\right]\right\}. \tag{27}$$

When $\alpha = 1$, equations (26) and (27) are reduced to the dispersion equation for the polygonal flow velocity profile (equation (12)), which appears commonly in the stability of hydrodynamic parallel flows [*Rayleigh*, 1880].

[15] Figure 3 shows $\gamma a/U_0$ as a function of ka for four density ratios α. The growth rate and wave number of the fastest growing mode decrease with an increase in α. When ρ_2 and $[dB_0/dx]_{x=a}$ are fixed in the magnetosphere, Figure 3 means that the growth rate decreases with an increase in the magnetosheath density (ρ_1), although increasing ρ_1 cannot completely stabilize the unstable K-H mode.

[16] Figure 4 shows $\omega_r a/U_0$ as a function of ka for four density ratios α in the range of ka, where $\gamma \ge 0$. The

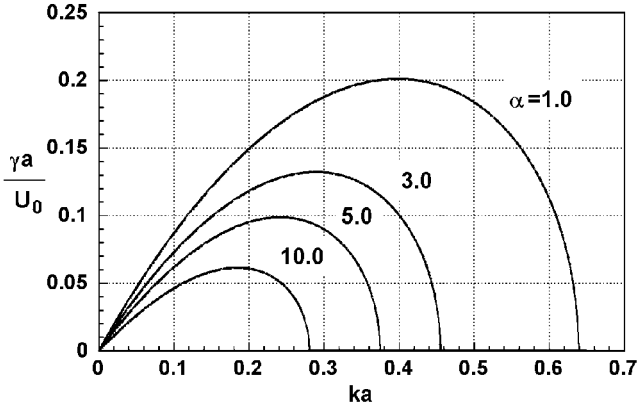

Figure 3. $\gamma a/U_0$ versus ka for four density ratios $\alpha = \rho_1/\rho_2$ = 1.0, 3.0, 5.0, 10.0.

negative value of ω_r means that the wave is propagating duskward. The magnitude of the normalized phase speed ω_r/kU_0 increases with a decrease in α. When $\alpha = 1.0$, the dispersion curve is a straight line and the wave is nondispersive. However, when $\alpha \neq 1.0$, the wave is dispersive.

5. Characteristics of Unstable Waves and Vortices

[17] If we assume $\alpha = \rho_1/\rho_2 = 3$, $n_0(x = a) = n_0$(magnetosphere) = 10^6 m^{-3}, $B_0(x_0) = B_0$(magnetosheath) = 30 nT as typical parameters of the dayside magnetopause [*Eastman and Hones*, 1979], we obtain the ion Larmor radius in the magnetosheath $\rho_{Li} \sim 131$ km. Since the magnetopause thickness is typically several times of ρ_{Li}, we assume $2a \sim 1000$ km, which is $\sim 7.6\ \rho_{Li}$. Then we obtain $U_0 = 19.9$ km/s. This smallness of U_0 compared with the solar wind bulk speed indicates that only the small portion around the stagnation point is subject to the present diamagnetically driven K-H instability for the magnetosheath field due north because the magnetosheath flow picks up quickly the tailward flow velocity ($\mathbf{E} \times \mathbf{B}$ drift) off the stagnation point in the equatorial plane. When the pressure gradient across the magnetopause becomes larger, a much wider region around the subsolar point becomes subject to the present K-H instability owing to an increase in U_0.

[18] Figure 3 shows that the fastest growing mode occurs at ka ~ 0.3 for $\alpha = 3$ and has $\gamma a/U_0 \sim 0.13$. Figure 4 shows $\omega_r a/U_0 \sim -0.21$ at ka ~ 0.3 for $\alpha = 3$. Therefore one obtains the wavelength of the fastest growing mode $\lambda_y \sim 10500$ km, the period of the fastest-growing mode $T = 2\pi/|\omega_r| = 751$ s, and the e-folding time of the fastest growing mode $\gamma^{-1} = 193$ s for $\alpha = 3$. These waves and vortices are propagating duskward ($\omega_r/k < 0$) in the direction of the ion diamagnetic drift with the phase velocity $\sim -0.7U_0 \sim -13.9$ km/s. Since the density ratio α is a variable parameter, let us calculate characteristics of waves for $\alpha = 10$. Figure 3 shows that the fastest growing mode occurs at ka ~ 0.2 for $\alpha = 10$ and has $\gamma a/U_0 \sim 0.06$. Figure 4 shows $\omega_r a/U_0 \sim -0.08$ at ka ~ 0.2 for $\alpha = 10$. Therefore one obtains the wavelength of the fastest growing mode $\lambda_y \sim 15700$ km, the period of the fastest growing mode $T = 2\pi/|\omega_r| = 1980$ s, and the e-folding time of the fastest growing mode $\gamma^{-1} = 419$ s for $\alpha = 10$. These waves and vortices are propagating duskward in the direction of the ion diamagnetic drift with the phase velocity $\sim -0.4U_0 \sim -7.96$ km/s.

[19] Since the ion diamagnetic drift at the subsolar magnetopause is duskward (see Figure 1) and the $\mathbf{E} \times \mathbf{B}$ drift in the flank magnetopause boundary is tailward for the magnetosheath field due north, the vortex created by the diamagnetically driven K-H instability near the subsolar region has the same rotational sense as the vortex created by the $\mathbf{E} \times \mathbf{B}$ shear driven K-H instability within the dusk flank boundary but has the opposite rotational sense to the vortex created by the $\mathbf{E} \times \mathbf{B}$ shear driven K-H instability within the dawn flank boundary.

6. Discussion

6.1. Nature of the Diamagnetically Driven K-H Instability

[20] The present instability is caused by the shear in the ion diamagnetic drift velocity and occurs for the flute mode ($\mathbf{k} \cdot \mathbf{B}_0 = 0$). It does not require a wave-particle interaction or resistivity. Therefore the present instability is not a drift instability and is essentially a fluid instability, which is destabilized by the shear in the macroscopic flow velocity arising from the nonideal MHD terms in the generalized Ohm's law (equation (1)). Although the ion diamagnetic drift velocity in equation (4) arises owing to the finite Larmor radius (FLR) effect of ions, the full FLR effects are not included in the present model. The full FLR effects for a suitable ordering can be incorporated in the present fluid model by including FLR terms (nondissipative gyroviscosity terms) in the divergence of the pressure tensor in the equation of motion. In order to make the present calculation more relevant to collisionless plasmas one would need to carry out the analysis kinetically by solving the ion gyrokinetic equation. A kinetic analysis would capture the special nature of the diamagnetic flow as a FLR effect. A kinetic treatment of the divergence of the pressure tensor and calculation of the pressure tensor using the solution of the linearized gyrokinetic equation would introduce new diamagnetic terms which do not appear in the present fluid treatment. Although the present theory has not

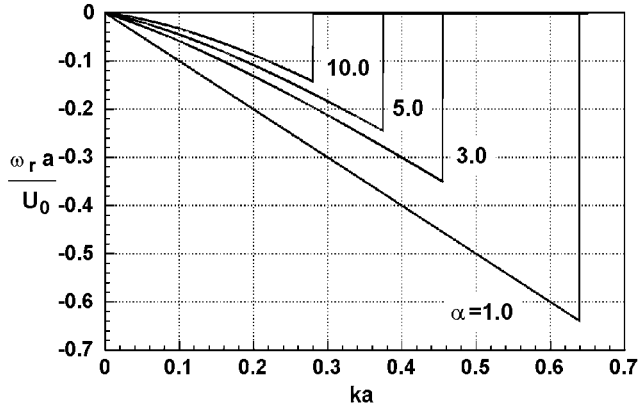

Figure 4. $\omega_r a/U_0$ versus ka for four density ratios $\alpha = \rho_1/\rho_2$ = 1.0, 3.0, 5.0, 10.0 in the range of ka, where $\gamma \geq 0$.

been developed to such a collisionless regime, *Lapenta and Brackbill* [2002] have shown the existence of the present instability in a collisionless plasma via a 2-D implicit particle in cell (PIC) simulation for the realistic mass ratio. They have investigated the development of kink modes in the 2-D plane perpendicular to the magnetic field in a Harris sheet. They have observed that the rapid development of a short wavelength, lower hybrid drift instability in the current sheet is followed by the slow development of long wavelength current sheet kinking. They calculated the growth rate and the wave number of the kink modes for the realistic mass ratio and found an excellent agreement between those obtained by simulation results and those calculated analytically for the present new K-H instability driven by the shear in the ion diamagnetic drift velocity [*Miura*, 2001]. Therefore even in collisionless plasmas, where the present fluid analysis is not strictly applicable, the existence of the present new K-H instability is indicated.

6.2. Relevance of the Subsolar Magnetopause Model to Observations

[21] The present model of the subsolar magnetopause shown in Figure 1 incorporates a general observed feature of increasing magnetic field strength and decreasing pressure toward the magnetosphere (*Eastman and Hones* [1979]; *Paschmann et al.*, [1993], Figure 9) satisfying the total pressure balance (see Figure 9 of *Paschmann et al.*, [1993]). Therefore the present simplified model of the subsolar magnetopause reflects average magnetic and thermal properties across the subsolar magnetopause. The present simplified model does not include the plasma depletion layer as observed on the magnetosheath side for the strongly northward magnetosheath field. However, the discontinuous density drop at $x = -a$ shown in Figure 1 and the corresponding temperature jump at $x = -a$ (not shown), so as to make $\rho_0 T_0$ constant, are consistent with the sharp drop in the density and the sharp rise in the temperature observed at the magnetopause, which are seen in the superposed epoch plots across the dayside magnetopause of *Paschmann et al.* [1993] (see their Figures 8 and 10).

6.3. Transport Processes by the K-H Instabilities

[22] A 2-D simulation of the ideal MHD K-H instability at the magnetopause, where ideal means $\mathbf{E} + \mathbf{v} \times \mathbf{B} = 0$, has shown that the anomalous transport of momentum and energy (but not mass) by Reynolds and Maxwell stresses into the magnetosphere is important in the nonlinear stage of the instability [*Miura*, 1984, 1992]. Such instability is expected most at the flank magnetopause. A single event analysis of *Owen and Slavin* [1992] and a statistical analysis of *Mist and Owen* [2002] of the distant tail plasma sheet have shown that the magnitude of the anomalous momentum flux (tangential stress) obtained by the simulation of the instability is within the range capable of explaining the slow tailward flows observed in the distant tail plasma sheet, which also drag and stretch tailward the closed magnetospheric field lines within the distant tail magnetopause.

[23] *Otto and Fairfield* [2000] showed by a 2-D MHD simulation that highly entangled field lines generated by the K-H instability for a configuration, where the wave vector of the perturbation has a component along the magnetic field direction, are subject to reconnection for a given current dependent resistivity. They suggested that the high-density filament of sheath origin generated by such a reconnection at the flank magnetopause is transported into the magnetosphere by an interchange motion. However, since their 2-D simulation does not allow the interchange motion, which is topologically possible only in 3-D, their 2-D simulation does not demonstrate such a net plasma transport. Two-dimensional hybrid simulations of $\mathbf{E} \times \mathbf{B}$ shear driven K-H instability in a uniform plasma [*Terasawa et al.*, 1992: *Fujimoto and Terasawa*, 1994] assume that the electrons are cold and a massless fluid. Therefore the electron fluid is frozen in to the magnetic field lines in their simulations ($\mathbf{E} + \mathbf{v}_e \times \mathbf{B} = 0$) and hence the electron fluid, which is frozen in to the magnetic field lines, cannot cross the magnetopause. Therefore the net plasma transport into the magnetosphere is not possible in their hybrid simulations, even if the density gradient is included, because the transport of both species of plasmas to satisfy the quasi-neutrality is not allowed. During the magnetosheath field due north there is a large velocity gradient due to $\mathbf{E} \times \mathbf{B}$ drift shear across the flank magnetopause in the equatorial plane, which destabilizes the $\mathbf{E} \times \mathbf{B}$ shear driven K-H instability and causes an efficient momentum transport. However, it is not certain whether the net plasma transport occurs by the $\mathbf{E} \times \mathbf{B}$ shear driven K-H instability at the flank boundary in the real 3-D configuration or whether possibly most plasmas outside the flank magnetopause are simply swept away tailward in the magnetosheath flow and do not cross the flank magnetopause into the magnetosphere.

[24] The present diamagnetically driven K-H instability may cause a macroscopic anomalous transport of plasmas into the magnetosphere, since the electron fluid is also not frozen in, i.e., $\mathbf{E} + \mathbf{v}_e \times \mathbf{B} + \nabla p_e/n\,e = 0$, which can be rewritten as

$$\mathbf{v}_{e\perp} = \frac{\mathbf{E} \times \mathbf{B}}{B^2} + \frac{1}{n\,e\,B^2}\mathbf{B} \times \nabla p_e. \tag{28}$$

We also note that the present diamagnetically driven K-H instability accompanies the parallel electric field $\delta E_z = \delta E_{||}$ when $k_z \neq 0$ owing to ∇p_e term in Ohm's law. Although both ion and electron fluids are not frozen-in to the magnetic field lines in the present K-H instability, the unfrozen-in parts of the unperturbed ion and electron fluid velocities are perpendicular to both $\mathbf{B}_0$ and ∇p_{i0} or both $\mathbf{B}_0$ and ∇p_{e0} (see equations (4) and (28), respectively) and both fluids do not cross the magnetopause in the present one-dimensional unperturbed state. Only in the perturbed state, is there a possibility of the plasma transport into the magnetosphere owing to nonlinearity. This possibility of the anomalous plasma transport should be further investigated by a 3-D analysis of the instability and simulations taking into account a possible parallel motion of electrons along the field line, so that the importance of the plasma transport by the diamagnetically driven K-H instability can be evaluated quantitatively.

[25] *Eastman and Christon* [1995] studied tracer ions (heavy ions only present in the solar wind) in situ near the dayside magnetopause and have shown that a net inward transport of the tracer ions occurred only for post-noon crossings and such transport was only observed within

about one hour of local noon. They also observed high variability in observed tracer ion density, which is inconsistent with any simple steady state transport process. *Eastman et al.* [1990] interpreted that this finite penetration of solar wind ions is due to finite ion FLR effects and acceleration along the polarization electric field, which is directed inward on the duskside magnetopause and outward on the dawnside magnetopause. However, this observation of the net transport near the subsolar region may not be inconsistent with the plasma transport near the subsolar region owing to the present diamagnetically driven K-H instability, because the distance along the equatorial magnetopause of about 1 hour of local noon can accommodate at least one wavelength of the fastest growing diamagnetically driven K-H mode λ_y = 10500 km−15700 km obtained in section 5 and thus allows the development of the diamagnetically driven K-H instablity. The very slow duskward vortex speed (8 km/s to 14 km/s) (or almost stagnant vortex near the subsolar magnetopause) may also be favorable to the local mass transport by this instability near the subsolar region.

6.4. A Dawn-Dusk Asymmetry of the K-H Instability

[26] The present study is limited to the subsolar region for the magnetosheath field due north, where the tailward $\mathbf{E} \times \mathbf{B}$ drift is negligible. However, since the total flow velocity is given by the sum of the $\mathbf{E} \times \mathbf{B}$ drift velocity and the ion diamagnetic drift velocity (see equation (4)), the ion diamagnetic drift at the magnetopause may cause a dawn-dusk asymmetry of the K-H instability when the present instability due to the shear in the ion diamagnetic drift velocity is extended to the dayside magnetopause off the noon meridian, where the tailward $\mathbf{E} \times \mathbf{B}$ drift is no longer negligible. Since the ion diamagnetic drift at the magnetopause is eastward, the ion diamagnetic drift velocity enhances the tailward $\mathbf{E} \times \mathbf{B}$ drift velocity in the dusk magnetopause boundary, but it reduces the tailward $\mathbf{E} \times \mathbf{B}$ drift velocity in the dawn magnetopause boundary. Therefore the present diamagnetically driven K-H instability may enhance the K-H instability on the duskside, but it may weaken the K-H instability on the dawnside. Thus the ion diamagnetic drift at the magnetopause may cause a dawn-dusk asymmetry of the strength of the K-H instability in the dayside magnetopause, although such an asymmetry is expected only in the front side magnetopause close to the subsolar region, when U_0 is much smaller than the bulk solar wind speed.

[27] *Wilber and Winglee* [1995] did a fully electromagnetic 2-D particle simulation of the K-H instability incorporating both electric field and pressure gradient at the flank boundaries and found dawn-dusk asymmetries. They found that the development of the K-H instability is stronger on the duskside than on the dawnside and that this dawn-dusk asymmetry is more evident when the ratio of ion Larmor radius to the boundary thickness is increased. While they observed familiar fluidlike vortex formation on the duskside, they found formation of thin filaments on the dawnside. These thin filaments are reminiscent of the hybrid simulation studies of *Thomas and Winske* [1993], which used a massless but a finite pressure electron fluid and found formation of coherent isolated structures on the order of the ion gyroradius by the K-H instability. *Wilber and Winglee* [1995] ascribed these dawn-dusk asymmetries to kinetic effects. However, at least the dawn-dusk asymmetry of the strength of the K-H instability may be ascribable to the existence of the ion diamagnetic drift velocity at the magnetopause boundary, i.e., a macroscopic fluid effect (nonideal MHD effect), which adds to the $\mathbf{E} \times \mathbf{B}$ drift velocity on the duskside and reduces it on the dawnside as explained above. Although they noticed the difficulty in separating mixing effects from heating effects in observed particle distribution, they found that observed changes in the particle distributions are mainly due to heating within the boundary layers, where sheared streaming flows are interacting, and are particularly strong in the dawnside boundary layers. Since the ion diamagnetic drift is counteracted by the $\mathbf{E} \times \mathbf{B}$ drift in the dawnside boundary, the $\mathbf{E} \times \mathbf{B}$ shear driven K-H instability is dominant in the dawnside boundary in their simulation model. Therefore their result may indicate that $\mathbf{E} \times \mathbf{B}$ shear driven K-H instability is inefficient in plasma transport in their configuration.

7. Summary

[28] The fact that the plasma motion is decoupled from that of the magnetic field due to nonideal MHD and that the electron fluid, although massless, is not frozen in owing to the ∇p_e term in equation (28), suggests that the present low-frequency diamagnetically driven K-H instability may cause a vortex assisted mass transport across the subsolar magnetopause in the plane perpendicular to the magnetic field. However, a further study of the three-dimensional effect (non-zero k_z and the parallel electron motion) on this instability and the nonlinear evolution of this instability is necessary to clarify consequences of this diamagnetically driven K-H instability in high-β space plasmas, in particular, to clarify its viability in plasma transport. When the present instability for the magnetosheath field due north is extended to the dayside magnetopause off the noon meridian, where the tailward $\mathbf{E} \times \mathbf{B}$ drift becomes important, the present K-H instability may enhance the K-H instability in the dusk magnetopause boundary and weaken the K-H instability in the dawn magnetopause boundary, because the ion diamagnetic drift velocity adds to the $\mathbf{E} \times \mathbf{B}$ drift on the duskside, whereas it reduces it on the dawnside. This dawn-dusk asymmetry (caused by the nonideal MHD effect) of the development of the K-H instability for the magnetosheath field due north, i.e., a stronger development of the K-H instability in the dusk magnetopause boundary than in the dawn magnetopause boundary, may explain the dawn-dusk asymmetry observed in a previous particle simulation study of the K-H instability.

[29] The 2-D nonideal MHD stability of a simplified model subsolar magnetopause under pressure balance for the magnetosheath field due north has been investigated by neglecting an unperturbed electric field and by retaining only the ion diamagnetic drift term in the drift velocity in equation (4), which is a nonideal MHD drift in a high-β plasma. The 2-D linear stability analysis has shown quantitatively the characteristics of unstable waves and vortices near the subsolar region and that the diamagnetically driven K-H instability is at least a viable instability for the magnetosheath field due north near the subsolar magneto-

pause, where there is a large ion pressure gradient, however, the high-β plasma dynamics have not been fully explored.

[30] **Acknowledgments.** This work was supported by Grants-in-Aid for Scientific Research 14540414. The computation portion of this work was supported by Radio Atmospheric Science Center of Kyoto University and Institute of Space and Astronautical Science as a joint research project. The computation for this work was performed at the computer center of the University of Tokyo.

[31] Lou-Chuang Lee thanks Fausto Gratton and another reviewer for their assistance in evaluating this paper.

References

Alfvén, H., Theories of the aurora, in *Proceedings of the Conference on Auroral Physics*, edited by N. C. Gerson, T. J. Keneshea, and R. J. Donaldson, p. 391, Air Force Cambridge Res. Cent., Cambridge, Mass., 1954.

Chandrasekhar, S., *Hydrodynamic and Hydromagnetic Stability*, Oxford Univ. Press, New York, 1961.

Eastman, T., and S. Christon, Ion composition and Transport near the earth's magnetopause, in *Physics of the Magnetopause*, *Geophysical Monogr. Ser.*, vol. 131, edited by P. Song, B. U. Ö. Sonnerup, and M. F. Thomsen, AGU, Washington D. C., 1995.

Eastman, T. E., and E. W. Hones Jr., Characteristics of the magnetospheric boundary layer and magnetopause layer as observed by Imp 6, *J. Geophys. Res.*, *84*, 2019, 1979.

Eastman, T. E., E. A. Greene, S. P. Christon, G. Gloeckler, D. C. Hamilton, and F. M. Ipavich, Ion composition in and near the frontside boundary layer, *Geophys. Res. Lett.*, *17*, 2031, 1990.

Fujimoto, M., and T. Terasawa, Ion inertia effect on the K-H instability, *J. Geophys. Res.*, *96*, 15,725, 1991.

Fujimoto, M., and T. Terasawa, Anomalous ion mixing within an MHD scale Kelvin-Helmholtz vortex, *J. Geophys. Res.*, *99*, 8601, 1994.

Hazeltine, R. D., and F. L. Waelbroeck, *The Framework of Plasma Physics*, Perseus, Reading, Mass., 1998.

Horton, W. T., T. Tajima, and T. Kamimura, Kelvin-Helmholtz instability and vortices in magnetized plasma, *Phys. Fluids*, *30*, 3485, 1987.

Huba, J. D., Hall dynamics of the Kelvin-Helmholtz instability, *Phys. Rev. Lett.*, *72*, 2033, 1994.

Lapenta, G., and J. U. Brackbill, Nonlinear evolution of the lower hybrid drift instability: Current sheet thinning and kinking, *Phys. Plasmas*, *9*, 1544, 2002.

Mist, R. T., and C. J. Owen, ISEE-3 observations of a viscously-driven plasma sheet: Magnetosheath mass and/or momentum transfer?, *Ann. Geophys.*, *20*, 619, 2002.

Miura, A., Anomalous transport by magnetohydrodynamic Kelvin-Helmholtz instabilities in the solar wind-magnetosphere interaction, *J. Geophys. Res.*, *89*, 801, 1984.

Miura, A., Kelvin-Helmholtz instability at the magnetospheric boundary: Dependence on the magnetosheath sonic Mach number, *J. Geophys. Res.*, *97*, 10,655, 1992.

Miura, A., Nonideal magnetohydrodynamic Kelvin-Helmholtz instability driven by the shear in the ion diamagnetic drift velocity in a high-β plasma, *Phys. Plasmas*, *8*, 5291, 2001.

Opp, E., and A. B. Hassam, Kelvin-Helmholtz instability in systems with large effective Larmor radius, *Phys. Fluids*, *B3*, 885, 1991.

Otto, A., and D. H. Fairfield, Kelvin-Helmholtz instability at the magnetotail boundary: MHD simulation and comparison with Geotail observations, *J. Geophys. Res.*, *105*, 21,175, 2000.

Owen, C. J., and J. A. Slavin, Viscously driven plasma flows in the deep geomagnetic tail, *Geophys. Res. Lett.*, *19*, 1443, 1992.

Paschmann, G., W. Baumjohann, N. Sckopke, and T.-D. Phan, Structure of the dayside magnetopause for low magnetic shear, *J. Geophys. Res.*, *98*, 13,409, 1993.

Pritchett, P. L., and F. V. Coroniti, The collisionless macroscopic Kelvin-Helmholtz instability, 1, Transverse electrostatic mode, *J. Geophys. Res.*, *89*, 168, 1984.

Rayleigh, J. W. S., On the stability, or instability, of certain fluid motions, *Proc. London Math. Soc.*, *11*, 57, 1880.

Tajima, T., W. Horton, P. J. Morrison, J. Schutkeker, T. Kamimura, K. Mima, and Y. Abe, Instabilities and vortex dynamics in shear flow of magnetized plasmas, *Phys. Fluids*, *B3*, 938, 1991.

Terasawa, T., M. Fujimoto, H. Karimabadi, and N. Omidi, Anomalous ion mixing within a Kelvin-Helmholtz vortex in a collisionless plasma, *Phys. Rev. Lett.*, *68*, 2778, 1992.

Thomas, V. A., and D. Winske, Kinetic simulation of the Kelvin-Helmholtz instability at the Venus ionopause, *Geophys. Res. Lett.*, *18*, 1943, 1991.

Thomas, V. A., and D. Winske, Kinetic simulations of the Kelvin-Helmholtz instability at the magnetopause, *J. Geophys. Res.*, *98*, 11,425, 1993.

Wilber, M., and R. M. Winglee, Dawn-dusk asymmetries in the low-latitude boundary layer arising from the Kelvin-Helmholtz instability: A particle simulation, *J. Geophys. Res.*, *100*, 1883, 1995.

Yoon, P. H., J. F. Drake, and A. T. Y. Lui, Theory and simulation of Kelvin-Helmholtz instability in the geomagnetic tail, *J. Geophys. Res.*, *101*, 27,327, 1996.

A. Miura, Department of Earth and Planetary Science, University of Tokyo, 7-3-1 Hongo, Bunkyo-ku, Tokyo 113-0033, Japan. (miura@yayoi.eps.s.u-tokyo.ac.jp)